

The Vaccination Threshold for SARS-CoV-2 Depends on the Indoor Setting and Room Ventilation

A. Mikszewski^{1,2}, L. Stabile³, G. Buonanno^{1,3}, L. Morawska*^{1,4}

¹ International Laboratory for Air Quality and Health, Queensland University of Technology, Brisbane, Qld, Australia

² CIUS Building Performance Lab, The City University of New York, New York, NY, USA, 10001

³ Department of Civil and Mechanical Engineering, University of Cassino and Southern Lazio, Cassino, FR, Italy

⁴ Global Centre for Clean Air Research (GCARE), Department of Civil and Environmental Engineering, Faculty of Engineering and Physical Sciences, University of Surrey, Guildford GU2 7XH, United Kingdom

*Corresponding Author: Professor Lidia Morawska, International Laboratory for Air Quality and Health, Queensland University of Technology, 2 George Street, Brisbane, Queensland 4001, Australia.

Email: l.morawska@qut.edu.au

Abstract

Background: Effective vaccines are now available for SARS-CoV-2 in the second year of the COVID-19 pandemic, but there remains significant uncertainty surrounding the necessary vaccination rate to safely lift occupancy controls in public buildings and return to pre-pandemic norms. The aim of this paper is to estimate setting-specific vaccination thresholds for SARS-CoV-2 to prevent sustained community transmission using classical principles of airborne contagion modeling. We calculated the airborne infection risk in three settings, a classroom, prison cell block, and restaurant, at typical ventilation rates, and then the expected number of infections resulting from this risk at varying levels of occupant susceptibility to infection.

Results: We estimate the vaccination threshold for control of SARS-CoV-2 to range from a low of 40% for a mechanically ventilation classroom to a high of 85% for a naturally ventilated restaurant. **Conclusions:** If vaccination rates are limited to a theoretical minimum of approximately two-thirds of the population, enhanced ventilation above minimum standards for acceptable air quality is needed to reduce the frequency and severity of SARS-CoV-2 superspreading events in high-risk indoor environments.

30 **Introduction**

31 Control of infectious disease is achieved when the average case does not beget another, and
32 transmission becomes sporadic in nature. For airborne contagion in shared indoor
33 atmospheres, Wells [1] established that the rate of transmission is inversely proportional to the
34 ventilation rate per susceptible occupant. It then follows that to control airborne contagion we
35 can either increase ventilation, or its equivalent through air filtration or disinfection, or
36 decrease the number of susceptible occupants through vaccination [2]. During the COVID-19
37 pandemic, lockdowns and occupancy controls have been widely applied to reduce transmission
38 of SARS-CoV-2. These are blunt but effective methods of increasing the ventilation rate per
39 susceptible occupant of indoor spaces. As SARS-CoV-2 vaccines become available to the public
40 in 2021, the question becomes: at what point is the number of susceptibles in public spaces low
41 enough so that occupancy limitations are no longer necessary to control the spread of the
42 virus?

43

44 To address this question, we must consider the primary settings of SARS-CoV-2 transmission. As
45 with other agents of airborne contagion such as *Mycobacterium tuberculosis*, SARS-CoV-2
46 thrives in congregate living and working spaces with shared air, such as prisons, schools,
47 restaurants, abattoirs, and care homes. The COVID-19 pandemic is also fueled by
48 superspreading events in crowded indoor environments where people vocalize and cannot
49 reliably wear masks. For example, Chang et al. [3] modeled full-service restaurants to produce
50 by far the largest increase in infections upon reopening after lockdown of any non-residential
51 location that people visit. Estimates of necessary vaccination rates for these high-risk
52 community settings should be protective in other microenvironments, and therefore
53 approximate a vaccination threshold to control SARS-CoV-2 such that the average case fails to
54 beget another.

55

56 The aim of this paper is to estimate setting-specific vaccination thresholds for SARS-CoV-2 using
57 classical principles of airborne contagion modeling. We included modeling scenarios for a

58 prison cell block and a full-service restaurant, two settings known to be high risk for SARS-CoV-2
59 transmission. To compare the vaccination threshold for SARS-CoV-2 to historical estimates for
60 measles virus, we also included a classroom scenario in our analysis. A secondary aim is to
61 quantify how vaccination and ventilation together reduce the pool of potential infectors in each
62 of the settings by estimating the minimum viral emission rate needed to reproduce infection at
63 varying levels of susceptibility.

64

65 **Materials and Methods**

66 *Approach and Definitions*

67 To develop our estimates, we defined a representative exposure scenario for each of the three
68 settings (classroom, prison, restaurant) involving one infectious occupant in a room of typical
69 geometry. We used an established airborne infection risk model to calculate the individual risk
70 of infection (R) for each susceptible occupant, and the event reproduction number (R_{event}) at
71 varying ventilation rates and number of susceptibles. R_{event} is the expected number of new
72 infections arising from a single infectious occupant at an event [4]. This is distinct from the basic
73 reproduction number (R_0), defined as the average number of new infections resulting from the
74 introduction of a single infectious individual into a fully (100%) susceptible host population [5].
75 For modeling purposes, we quantified the number of susceptibles as the percent of the total
76 occupants who are susceptible to infection (i.e., not successfully vaccinated or immune from
77 prior infection). We use the term area concentration of susceptibles to represent the area of
78 indoor space (square meters [m^2]) per susceptible occupant. The threshold number of
79 susceptibles and the threshold area concentration of susceptibles occur at a calculated R_{event} of
80 one, above which one case begets more than another. For each setting we calculated these
81 two threshold values at a mechanical ventilation rate based on American National Standards
82 Institute (ANSI)/American Society of Heating, Refrigerating and Air-Conditioning Engineers
83 (ASHRAE) 62.1 standards for acceptable air quality [6], and at a natural ventilation rate when
84 windows cannot be opened and air exchange results solely from infiltration through the
85 building envelope. We then determined the vaccination threshold as the complement of the

86 threshold number of susceptibles assuming no immunity from prior infection. For comparative
87 purposes, we also calculated the threshold values in each setting at a ventilation rate of 15
88 liters per second per person ($L\ s^{-1}\ p^{-1}$), a typical goal for high indoor air quality consistent with
89 EN 15251 Category I criteria for a non low polluting building [7].

90

91 *Calculation of the Event Reproduction Number (R_{event})*

92 We used the Gammaitoni and Nucci [8] equation coupled with a Poisson dose-response model
93 to calculate R_{event} for SARS-CoV-2 in a prototypical classroom, prison cell block, and full-service
94 restaurant. The first step is calculating the probability of infection (P_I) resulting from each
95 exposure through equations (1-3):

96

$$97 n(t, ER_q) = \frac{ER_q \cdot I}{IVRR \cdot V} \cdot (1 - e^{-IVRR \cdot t}) \quad (\text{quanta m}^{-3}) \quad (1)$$

98

$$99 D_q(ER_q) = IR \int_0^T n(t) dt \quad (\text{quanta}) \quad (2)$$

100

$$101 P_I = 1 - e^{-D_q} \quad (\%) \quad (3)$$

102

103 Where n represents the quanta (infectious dose for 63% of susceptible occupants by droplet
104 nuclei inhalation) concentration in air at time t , ER_q is the quanta emission rate (quanta h^{-1}), I is
105 the number of infectious occupants (assumed to be only one), V is the volume of the indoor
106 environment considered (m^3), $IVRR$ (h^{-1}) represents the infectious virus removal rate in the
107 space investigated, D_q is the dose of quanta inhaled by susceptible occupants, T is the total time
108 of the exposure (h), and P_I is the probability of infection of a susceptible occupant. The
109 infectious virus removal rate is the sum of the air exchange rate (AER) via ventilation in units of
110 air changes per hour, the particle deposition on surfaces (k_d , e.g. via gravitational settling), and
111 the viral inactivation in ambient air (λ).

112

113 With all other parameters held constant, the probability of infection calculated in equation (3)
114 assumes different values based on ER_q . To evaluate the individual risk (R) of infection of an
115 exposed susceptible occupant for a given exposure scenario, we then quantify the probability of
116 infection as a function of ER_q ($P_I[ER_q]$) and the probability of occurrence of each ER_q value (P_{ERq})
117 which can be defined by the probability density function (pdf_{ERq}) of ER_q assuming a lognormal
118 distribution. Since the probability of infection ($P_I[ER_q]$) and the probability of occurrence P_{ERq}
119 are independent events, R for a given ER_q , $R(ER_q)$, can be evaluated as the product of the two
120 terms:

121

122
$$R(ER_q) = P_I(ER_q) \cdot P_{ERq} \quad (4)$$

123

124 where $P_I(ER_q)$ is the conditional probability of the infection, given a certain ER_q , and P_{ERq}
125 represents the relative frequency of the specific ER_q value. The individual risk (R) of an exposed
126 susceptible occupant is then calculated by integrating the pdf_R for all possible ER_q values, i.e.
127 summing up the $R(ER_q)$ values calculated in eq. (5):

128

129
$$R = \int_{ER_q} R(ER_q) dER_q = \int_{ER_q} (P_I(ER_q) \cdot P_{ERq}) dER_q \quad (5)$$

130

131 Equation (5) represents a numerical solution approximately equaling the average P_I that would
132 result from a Monte Carlo simulation randomly sampling ER_q from its lognormal distribution.
133 The individual risk R also represents the ratio between the number of new infections and the
134 number of exposed susceptible occupants (S) for a given exposure scenario and considering all
135 possible ER_q values from its lognormal distribution for the infectious occupant under
136 investigation. For a single exposure event involving a single infectious occupant, R_{event} is
137 calculated as the product of R and S as in eq. (6):

138

139
$$R_{event} = R \cdot S \quad (infections) \quad (6)$$

140

141 For a specific event, the threshold number of susceptibles occurs at the value of S where R_{event}
142 equals one ($S_{\text{threshold}} = 1/R$) and is calculated by dividing $S_{\text{threshold}}$ by the total room occupancy
143 less the infected occupant. The threshold area concentration of susceptibles is calculated by
144 dividing $S_{\text{threshold}}$ by the room area.

145

146 *Modeling Scenario Input Parameters*

147 Input parameters for the classroom, prison, and restaurant scenarios are summarized in Table
148 1. Geometry and default occupancy for the classroom are based on the rooms studied by Wells
149 [1] with an exposure time of 5.5 hours representing a single day. The restaurant model
150 encompasses the dining room geometry of the US Department of Energy building prototype for
151 a full-service restaurant, with an exposure time of 1.5 hours [9]. The prison model is based on
152 the largest cell block size studied by Hoge et al. [10], which was overcrowded with a median
153 living area of 3.2 m^2 per inmate. The exposure time for the prison scenario is likely highly
154 variable, but we assume it to be 36 hours since inmates share the same airspace for extended
155 time periods and peak infectiousness has been estimated to occur at 2 days before to 1 day
156 after symptom onset [11]. Thus, a 36-hour period where infectiousness is at or near peak but
157 without symptoms that would prompt quarantine can be reasonably expected.

158

159 The distributions for the quanta emission rate were modified from Buonanno et al. [12; see
160 Supplemental Material] for standing and speaking for the classroom (assuming the class
161 instructor is the emitting subject), resting and loudly speaking for the restaurant, and resting
162 and oral breathing for the prison, with the \log_{10} average ER_q values indicated in Table 1 and a
163 \log_{10} standard deviation for all distributions of 1.2. All susceptible occupants were assumed to
164 be at rest with an inhalation rate of $0.49 \text{ m}^3 \text{ h}^{-1}$. We used a deposition rate, k_d , of 0.24 h^{-1} based
165 on the ratio between the settling velocity of super-micrometer particles (roughly $1.0 \times 10^{-4} \text{ m s}^{-1}$
166 [13]) and the height of the emission source (1.5 m). For the SARS-CoV-2 inactivation rate in air,
167 we used a value of 0.63 h^{-1} based on the measurements reported by van Doremalen et al. [14].

168 For each scenario, we varied the AER from zero to a maximum of six air changes per hour to
169 calculate R and R_{event} at a number of susceptibles ranging from 0-100%.

170

171 **Table 1.** Modeling input and ventilation reference parameters

172

	Classroom	Prison	Restaurant	Average
Room Volume (m^3)	170	576	640	462
Room Area (m^2)	57	160	213	143
Occupancy (Persons)	20	50	100	57
Occupancy ($m^2 \text{ Person}^{-1}$)	2.8	3.2	2.1	2.7
Exposure Time (h)	5.5	36	1.5	14
Infectious Occupant Activity	Standing, speaking	Resting, oral breathing	Resting, loudly speaking	--
Median $ER_q \log_{10}$ (quanta h^{-1})	0.41	-0.28	1.2	0.44
Natural Ventilation AER (h^{-1})	0.5	0.5	0.5	0.5
Mechanical Ventilation AER (h^{-1})	2.6	1.4	3.2	2.4
High Air Quality AER (h^{-1})	6.4	4.7	8.4	6.5
Natural Ventilation ($L s^{-1} p^{-1}$)	1.2	1.6	0.89	1.2
Mechanical Ventilation ($L s^{-1} p^{-1}$)	6.1	4.4	5.7	5.4
High Air Quality Ventilation ($L s^{-1} p^{-1}$)	15	15	15	15

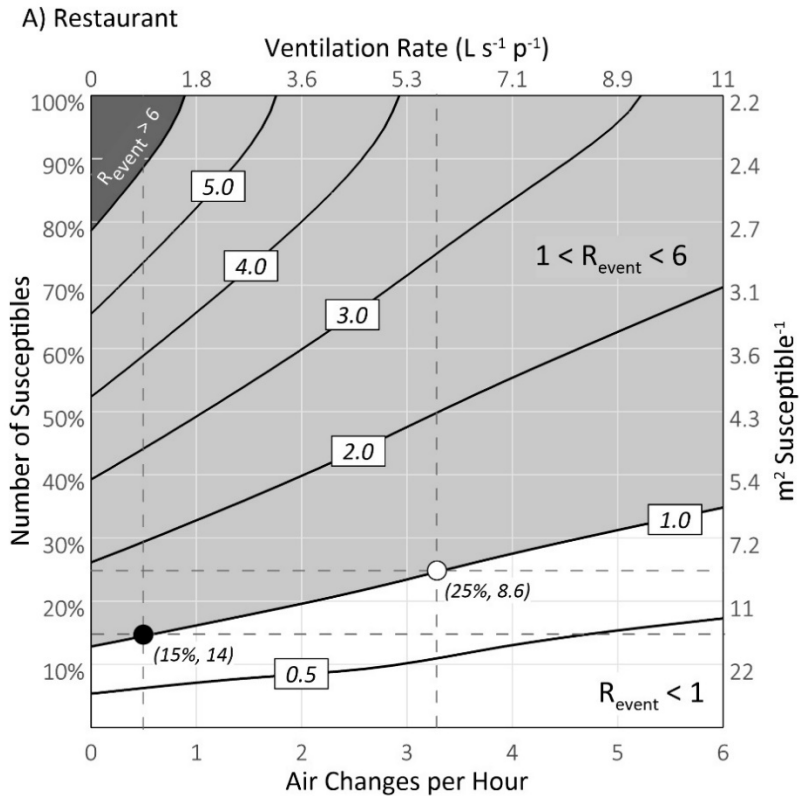
173

174 Results

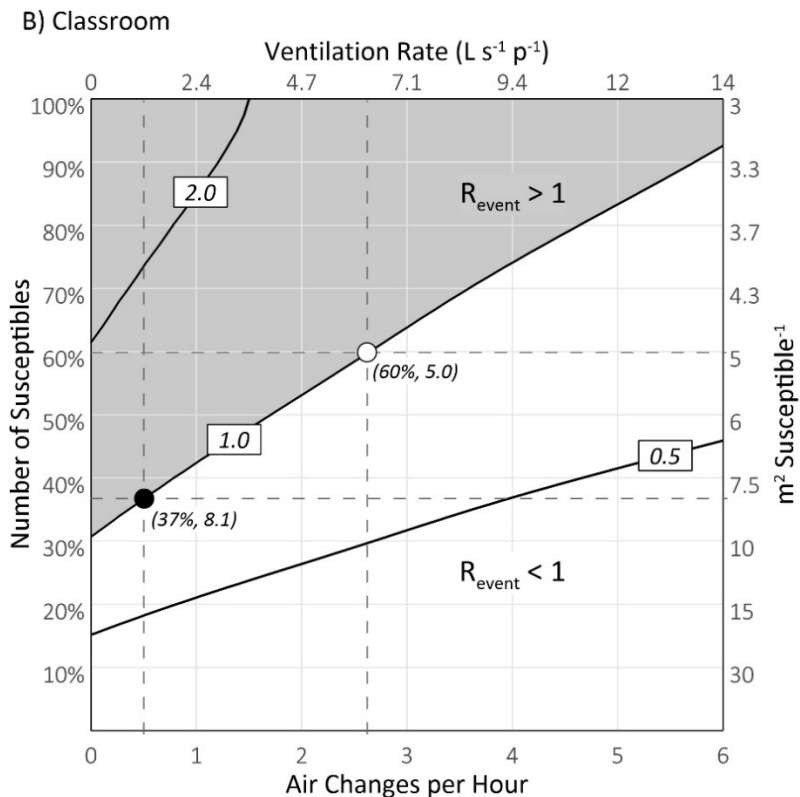
175 The results of our modeling analysis are summarized in Figure 1 and Table 2 for each setting at
176 an assumed natural ventilation rate of 0.5 air changes per hour, and at a mechanical ventilation
177 rate corresponding to the applicable standard for acceptable air quality based on ANSI/ASHRAE
178 62.1 and shown in Table 1 [6]. The naturally ventilated restaurant (Figure 1A) has the lowest
179 threshold number of susceptibles of 15%, and the mechanically ventilated classroom (Figure
180 1B) has the highest threshold number of susceptibles of 60%. The threshold number of
181 susceptibles for the prison cell block (Figure 1C) exhibits the smallest difference between the
182 natural ventilation (23%) and mechanical ventilation (31%) scenarios.

183

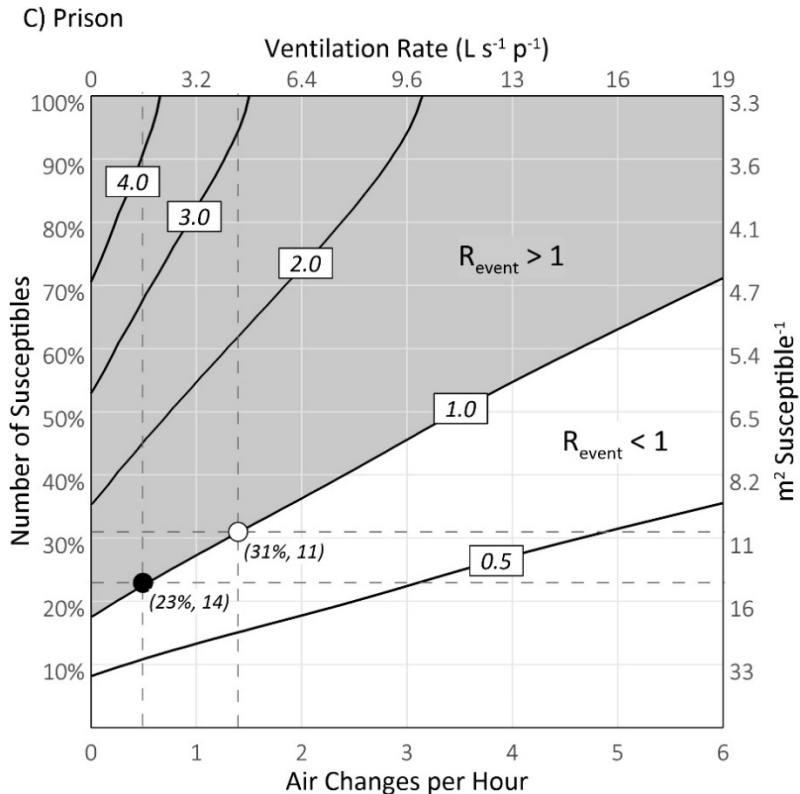
184 **Figure 1**



185



186



187

188

189 **Figure 1 Caption.** Surface graphs of R_{event} for SARS-CoV-2 as a function of the number of
190 susceptibles and air exchange rate (AER) for the restaurant (A), classroom (B) and prison cell
191 block (C) modeling scenarios. Contour lines connect equal R_{event} values. The black- and white-
192 filled points along the $R_{event} = 1.0$ contour line identify the threshold number of susceptibles for
193 natural ventilation and mechanical ventilation scenarios, respectively, at the intersection of the
194 dashed horizontal and vertical lines. The threshold values are labeled in parenthesis in terms of
195 both the percent susceptible and $m^2 \text{ susceptible}^{-1}$.

196

197
198

Table 2. Modeling results

	Ventilation	Classroom	Prison	Restaurant	Average
Individual Risk (R) (%)	Natural	14%	8.9%	6.8%	9.9%
	Mechanical	8.8%	6.5%	4.1%	6.5%
	High Air Quality	5.5%	3.4%	2.3%	3.7%
Threshold Number of Susceptibles (%)	Natural	37%	23%	15%	25%
	Mechanical	60%	31%	25%	39%
	High Air Quality	95%	60%	44%	66%
Threshold Area Concentration (m^2 Susceptible $^{-1}$)	Natural	8.1	14	14	12
	Mechanical	5.0	11	8.6	8.2
	High Air Quality	3.1	5.4	4.9	4.5

199
200 The average threshold number of susceptibles for all three settings calculated under the natural
201 and mechanical ventilation rates is 32%. In the absence of immunity from prior infections and
202 assuming vaccination confers complete protection, these results suggest an average vaccination
203 threshold of 68% with a range of 40-85%. The naturally ventilated prison and restaurant have
204 the highest threshold area concentration of susceptibles at $14 \text{ m}^2 \text{ susceptible}^{-1}$, while the
205 mechanically ventilated classroom has the lowest at approximately $5.0 \text{ m}^2 \text{ susceptible}^{-1}$. The
206 overall average threshold area concentration of susceptibles for mechanical and natural
207 ventilation is approximately $10 \text{ m}^2 \text{ susceptible}^{-1}$.

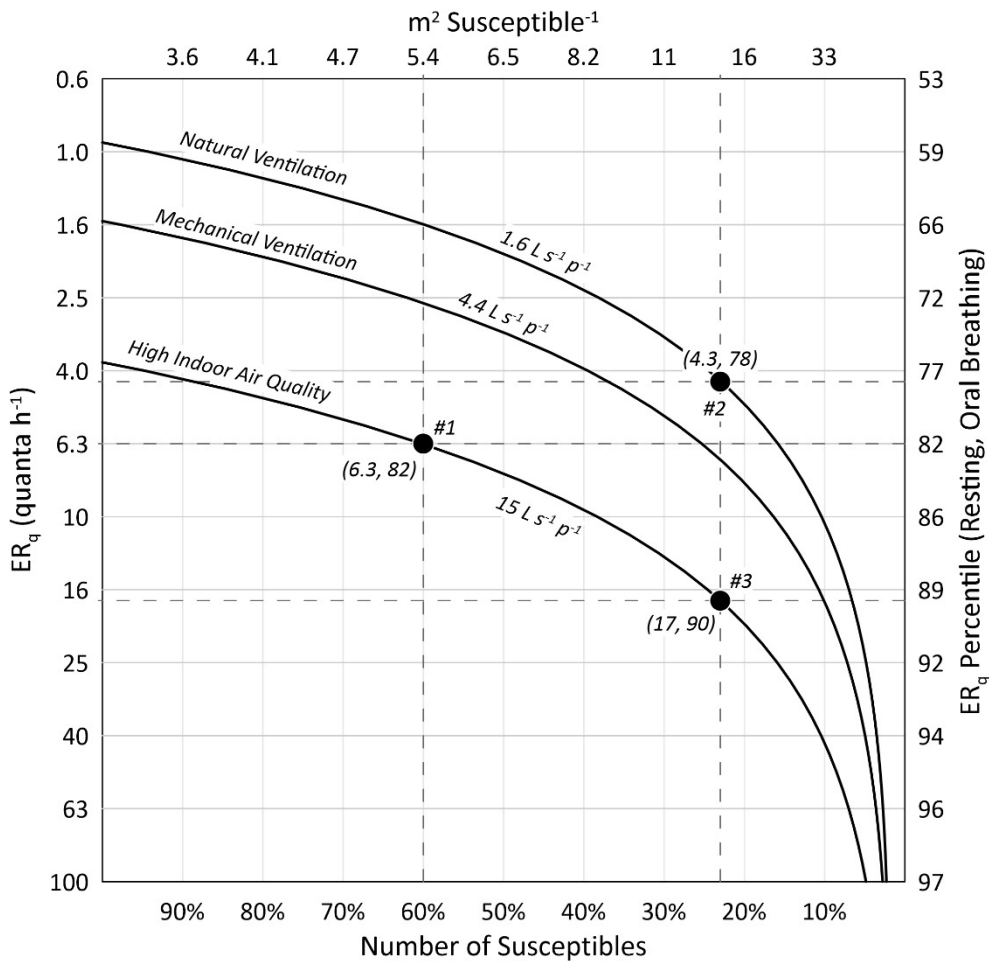
208
209 Increasing the ventilation rate to the high air quality metric of $15 \text{ L s}^{-1} \text{ p}^{-1}$ increases the
210 threshold
211 number of susceptibles to 95% in the classroom, 60% in the prison, and 44% in the restaurant.
212 The average threshold number of susceptibles for all three settings becomes 66%, more than
213 twice the average of the natural and mechanical ventilation scenarios. To maintain an R_{event} of
214 one in a fully susceptible population, the estimated ventilation requirements are $43 \text{ L s}^{-1} \text{ p}^{-1}$ (24
215 air changes per hour), $30 \text{ L s}^{-1} \text{ p}^{-1}$ (9.5 air changes per hour) and $17 \text{ L s}^{-1} \text{ p}^{-1}$ (7.0 air changes per
216 hour) for the restaurant, prison, and classroom, respectively. Such high air exchange rates are
217 impracticable in many settings, suggesting a role for ultraviolet air disinfection [15, 16].

218
219 Increasing ventilation and/or decreasing the number of susceptibles has the effect of increasing
220 the minimum ER_q necessary to produce an R_{event} of one, thereby reducing the number of
221 infected occupants capable of infecting others on average. This is illustrated in Figure 2 for the
222 prison cell block model. For the naturally ventilated cell block in a fully susceptible population,
223 the minimum ER_q is just below $1.0 \text{ quanta h}^{-1}$, occurring at the 58th percentile value of the
224 resting, oral breathing distribution. At a number of susceptibles of 23%, the minimum ER_q
225 becomes approximately $4.3 \text{ quanta h}^{-1}$ at the 78th percentile value. Increasing ventilation to 15
226 $\text{L s}^{-1} \text{ p}^{-1}$ further decreases the pool of potential infectors, raising the minimum ER_q to

227 approximately 17 quanta h⁻¹ at the 90th percentile value, indicating only a 10% chance of a
228 secondary infection.

229

230 **Figure 2**



231
232

233 **Figure 2 Caption.** Minimum quanta emission rates (ER_q) for $R_{event} \geq 1.0$ for the prison scenario
234 under natural ventilation, mechanical ventilation, and high air quality ventilation conditions as a
235 function of the number of susceptibles. Points #1 and #2 identify the minimum emission rates
236 for high air quality ventilation and natural ventilation at their respective threshold number of
237 susceptibles from Figure 1C. Point #3 identifies the minimum emission rate for high air quality
238 ventilation at the natural ventilation threshold number of susceptibles, representing both high
239 ventilation and high vaccination. The minimum emission values are labeled in parenthesis,
240 denoting the emission in quanta h^{-1} and its corresponding percentile in the resting, oral
241 breathing ER_q distribution.

242

243 **Discussion**

244 The overall average threshold number of susceptibles calculated for the natural and mechanical
245 ventilation scenarios is 32%, suggesting a basic reproduction number (R_0) of approximately 3 in
246 accordance with general epidemiological theory that the equilibrium susceptible fraction in a
247 host population is the reciprocal of R_0 [5]. This is consistent with R_0 estimates for the initial
248 SARS-CoV-2 outbreaks in Wuhan, China and Northern Italy [17]. Our analysis is also consistent
249 with the overdispersed epidemiological nature of SARS-CoV-2 [18], with a minority of cases
250 accounting for most secondary transmissions. In the naturally ventilated prison, we calculate
251 that emissions approximately below the 60th percentile value will fail to reproduce infection, on
252 average, indicating the median emission is not a significant source of transmission (Figure 2).
253 Furthermore, application of equation (5) for the prison scenario shows that emissions above
254 the 80th percentile value account for at least 85% of the total individual risk, suggesting a
255 dispersion parameter (k) between 0.10 and 0.16. This derivation is provided in the
256 Supplemental Material and enables quantification of the probability of SARS-CoV-2
257 superspreading and outbreak extinction as defined by Lloyd-Smith et al. [19]. Due to this
258 overdispersion, vaccinating 77% of inmates in a naturally ventilated cell block still leaves the
259 remaining susceptible population vulnerable to emitters above the 78th percentile. As a result,
260 explosive but comparatively rare superspreading events may continue in crowded, poorly
261 ventilated settings, a phenomenon that challenges the eradication of measles virus [20].
262

263 Applying both high vaccination and high ventilation raises both the threshold number of
264 susceptibles and the minimum emission rate needed to reproduce infection, decreasing the
265 dispersion parameter and increasing the probability of outbreak extinction. Uniformly
266 increasing ventilation to a high air indoor air quality metric of $15 \text{ L s}^{-1} \text{ p}^{-1}$ approximately doubles
267 the average threshold number of susceptibles and therefore halves vaccination requirements
268 for equivalent prevention of infection. Thus, while a ventilation rate of $15 \text{ L s}^{-1} \text{ p}^{-1}$ is unlikely to
269 prevent all secondary infections when a high-emitting index case is introduced into a fully
270 susceptible, indoor population [21], it can provide a substantial downstream epidemiological

271 benefit relative to a poorly ventilated baseline condition. This effect is important for pathogens
272 where transmission is overdispersed, with *Mycobacterium tuberculosis* being another example
273 [22], as superspreading events (SSEs) facilitate infection of the high-emitting minority that
274 continues the chain of contagion. For our prison cell block model, we estimate that increasing
275 the natural ventilation rate to the high air quality ventilation rate decreases the SSE probability
276 from 16% to 6.6% (see Supplemental Material). This is an important finding, as prisons and jails
277 are clear hot spots for SARS-CoV-2 transmission. For example, by March 2021, five California
278 State Prisons (Chuckawalla Valley, California Rehabilitation Center, Avenal, San Quentin, and
279 California Men's Colony) reported total confirmed COVID-19 case rates above 800 per 1,000
280 inmates [23]. Such high case rates imply a low threshold number of susceptibles, with
281 inadequate ventilation a likely factor. Indeed, during an investigation of the San Quentin State
282 Prison in June 2020, McCoy et al. [24] noted cell blocks with windows that were welded shut
283 and with fan systems that appeared to have been inactive for years.

284
285 Historical examples for measles virus illustrating the relationship between ventilation and the
286 threshold number of susceptibles in classrooms are provided by Wells [1, 25] and Thomas [26].
287 In classic experiments using upper-room air irradiation in primary and upper school classrooms
288 during the 1941 outbreak of measles in suburban Philadelphia, USA, Wells estimated a
289 threshold number of susceptibles of approximately 20% in unirradiated rooms at a then-
290 standard ventilation rate of $14 \text{ L s}^{-1} \text{ p}^{-1}$. Irradiated classrooms supported a much higher
291 threshold number of susceptibles of approximately 57% because the weekly probability of
292 infection in the irradiated rooms was approximately four to five times lower than in the
293 unirradiated rooms [1, 25]. The findings of Wells are similar to those of Thomas [26] who
294 studied the spread of measles in primary schools in the Woolwich district of London in 1904.
295 Thomas concluded that outbreaks of measles tend to occur when the number of susceptibles
296 exceeds approximately 33% and generally continue until the proportion is reduced to 18%.
297 However, the spread of measles in the Woolwich classrooms below the 33% threshold was
298 highly heterogeneous, with many experiencing significant outbreaks infecting a majority of

299 susceptible occupants. The three classes with a number of susceptibles below 10% experienced
300 zero cases of measles, and two temporary schools with crowding and poor ventilation had
301 explosive outbreaks that nearly exhausted the population of susceptibles, with a median
302 probability of infection of 87% for the five classes in the two schools. Thomas measured a
303 carbon dioxide (CO_2) concentration of 3,000 parts per million in one of the temporary schools
304 [26], indicating a steady-state ventilation rate below $2 \text{ L s}^{-1} \text{ p}^{-1}$ and comparable to our natural
305 ventilation scenario. The higher contagiousness of measles as compared to SARS-CoV-2 is
306 illustrated by the historical reported threshold number of susceptibles of 20-33% as compared
307 to our classroom estimate of 37-60% despite the lower ventilation standards of present day.
308 This difference is also reflected by the median classroom measles probability of infection of
309 87% for the poorly ventilated temporary schools studied by Thomas [26] as compared to the
310 individual risk (R) of approximately 14% we calculated for SARS-CoV-2 (Table 2). A ventilation
311 rate of $14 \text{ L s}^{-1} \text{ p}^{-1}$ appears sufficient, on average, to prevent sustained airborne transmission of
312 SARS-CoV-2 in a classroom with a number of susceptibles up to approximately 90%.

313
314 A limitation of our infection risk modeling approach is the assumption of a homogeneous
315 concentration of droplet nuclei within the room, with viral emissions being instantaneously and
316 completely mixed. However, a recent comparison of this box-modeling approach with
317 computational fluid dynamics (CFD) simulations for a classroom environment indicates
318 relatively minor errors for natural (6%) and forced mechanical (29%) ventilation scenarios [27].
319 The uncertainty in the emission rate, based on viral loads that vary several orders of magnitude
320 between individuals and over time [28], is likely much more significant than that caused by
321 incomplete mixing at the small scale of our models. Further improvements to the emission rate
322 distributions are needed that incorporate variation in droplet volume concentrations [28, 29],
323 such that a more complete stochastic emission model can be implemented. An additional
324 limitation is our estimation of vaccination thresholds using singular, setting-specific events,
325 without considering cumulative exposure effects that may result from an infectious person
326 attending class in two successive days, for example. The importance of singular SSEs on SARS-

327 CoV-2 transmission is well established, and such events likely occur during a narrow 1-2 day
328 window of peak infectivity [30]. As such we do not expect cumulative exposures to be a
329 significant factor outside of co-habitation environments, which is why our prison scenario used
330 a 36-hour duration. Our approach also does not account for extreme examples such as
331 someone visiting multiple similar restaurants for similar durations on the same evening (thus
332 increasing the number of exposed susceptibles to a similar infectious dose), or for a bartender
333 or other vocalizing restaurant employee who may be present for much longer than 1.5 hours.
334 Indeed, there are numerous other scenarios, such as choirs or high-intensity exercise rooms,
335 where higher vaccination thresholds are likely, reinforcing the need for high levels of both
336 vaccination and ventilation also considering that vaccines are not 100% protective.

337

338 **Conclusions**

339 Our fully prospective airborne infection modeling results are consistent with the transmission
340 dynamics of SARS-CoV-2 and illustrate the challenges presented by substantial heterogeneity in
341 the settings of contagion and a skewed viral emission rate distribution. To support pre-
342 pandemic levels of occupancy, required vaccination rates are much higher for a naturally
343 ventilated restaurant (85%) than for a mechanically ventilated classroom (40%). As vaccination
344 campaigns progress it follows that occupancy limitations should be relaxed for classrooms
345 before full-service indoor restaurants. Maintaining focus on enhanced ventilation together
346 with vaccination is especially important considering the emergence of new SARS-CoV-2 strains
347 that are more contagious with increasing possibility of second infections or vaccine
348 breakthrough infections. Avoidance of overcrowding remains a critical strategy to minimize
349 airborne transmission, as our calculations suggest ensuring an average of 10 m^2 per susceptible
350 occupant of an indoor space is approximately equivalent to achieving a number of susceptibles
351 of 32% of normal occupancy. This is because the ventilation rate per susceptible occupant is
352 more than tripled relative to the baseline average occupant loading of 2.7 m^2 per susceptible
353 occupant for the three settings evaluated herein.

354

355 **Declarations**

356 **Ethics approval and consent to participate:** Not applicable

357 **Consent for publication:** Not applicable

358 **Availability of data and materials:** All data generated or analysed during this study are included
359 in this published article and its supplementary information file.

360 **Competing interests:** The authors have no conflicts or competing interests to disclose.

361 **Funding:** This manuscript was prepared without external funding.

362 **Authors' contributions:** AM, LS, GB, LM designed research; AM performed research; AM, LS,
363 GB, LM analyzed data; AM wrote the paper; and LS, GB, LM reviewed the paper

364 **Acknowledgements:** The authors thanks Chantal Labb  at QUT ILAQH for her invaluable
365 research support.

366

367 **References**

- 368 1. Wells WF. Airborne Contagion and Air Hygiene. Cambridge, Mass.: Harvard University Press,
369 1955.
- 370
- 371 2. Riley RL. Prevention and Control of Airborne Infection in the Community. In: Annals of the
372 New York Academy of Sciences. Airborne Contagion. Vol 353. USA: The New York Academy
373 of Sciences, 1980:331-339.
- 374
- 375 3. Chang S, Pierson E, Koh PW, et al. Mobility network models of COVID-19 explain inequities
376 and inform reopening. *Nature*. 2021;589:82–87.
- 377
- 378 4. Tupper P, Boury H, Yerlanov M, Colijn C. Event-specific interventions to minimize COVID-19
379 transmission. *Proc Natl Acad Sci USA*. 2020;117:32038-32045..
- 380
- 381 5. Anderson RM, May RM. Infectious Diseases of Humans: Dynamics and Control. New York:
382 Oxford University Press, 1991.
- 383
- 384 6. ASHRAE, ANSI/ASHRAE Standard 62.1-2019. Ventilation for acceptable indoor air quality.
385 Atlanta, GA: American Society of Heating, Refrigerating, and Air-Conditioning Engineers,
386 Inc.; 2019:92.
- 387
- 388 7. EN 15251. Indoor environmental input parameters for design and assessment of energy
389 performance of buildings addressing indoor air quality, thermal environment, lighting and
390 acoustics. CEN 2007, Brussels.
- 391
- 392 8. Gammaitoni L, Nucci MC. Using a mathematical model to evaluate the efficacy of TB control
393 measures. *Emerg Infect Dis*. 1997;3(3):335-342.
- 394

- 395 9. Thornton BA, Rosenberg MI, Richman EE, et al. Achieving the 30% Goal: Energy and Cost
396 Savings Analysis of ASHRAE Standard 90.1-2010. Pacific Northwest National Laboratory
397 (PNNL): Richland, WA; 2011:PNNL-20405
398
- 401 10. Hoge CW, Reichler MR, Dominguez EA, et al. An epidemic of pneumococcal disease in an
400 overcrowded, inadequately ventilated jail. *N Engl J Med.* 1994;331(10):643-648.
404
- 402 11. He X, Lau EHY, Wu P, et al. Author Correction: Temporal dynamics in viral shedding and
403 transmissibility of COVID-19. *Nat Med.* 2020;26:1491–1493.
408
- 405 12. Buonanno G, Morawska L, Stabile L. Quantitative assessment of the risk of airborne
406 transmission of SARS-CoV-2 infection: Prospective and retrospective applications. *Environ
407 Int.* 2020;145:106112.
412
- 409 13. Chatoutsidou SE, Lazaridis M. Assessment of the impact of particulate dry deposition on
410 soiling of indoor cultural heritage objects found in churches and museums/libraries. *J Cult
411 Herit.* 2019;39:221–228.
415
- 413 14. van Doremalen N, Bushmaker T, Morris DH, et al. Aerosol and surface stability of SARS-CoV-
414 2 as compared with SARS-CoV-1. *N Engl J Med.* 2020;382(16):1564-1567.
418
- 416 15. Riley RL, Nardell EA. Clearing the air. The theory and application of ultraviolet air
417 disinfection. *Am Rev Respir Dis.* 1989;139(5):1286-1294.
421
- 419 16. Nardell EA, Nathavitharana RR. Airborne spread of SARS-CoV-2 and a potential role for air
420 disinfection. *JAMA.* 2020;324(2):141–142.

- 422 17. D'Arienzo M, Coniglio A. Assessment of the SARS-CoV-2 basic reproduction number, R₀,
423 based on the early phase of COVID-19 outbreak in Italy. *Biosaf Health*. 2020;2(2):57-59.
- 424
- 425 18. Adam DC, Wu P, Wong JY, et al. Clustering and superspreading potential of SARS-CoV-2
426 infections in Hong Kong. *Nat Med*. 2020;26:1714–1719.
- 427
- 428 19. Lloyd-Smith JO, Schreiber SJ, Kopp PE, et al. Superspreading and the effect of individual
429 variation on disease emergence. *Nature*. 2005;438(7066):355–359.
- 430
- 431 20. Langmuir AD. Changing Concepts of Airborne Infection of Acute Contagious Diseases: A
432 Reconsideration of Classic Epidemiologic Theories. In: Annals of the New York Academy of
433 Sciences. *Airborne Contagion*. Vol 353. USA: The New York Academy of Sciences;1980:35-
434 44.
- 435
- 436 21. Nardell EA, Keegan J, Cheney SA, Etkind SC. Airborne infection. Theoretical limits of
437 protection achievable by building ventilation. *Am Rev Respir Dis*. 1991;144(2):302-306.
- 438
- 439 22. Melsew YA, Gambhir M, Cheng AC, et al. The role of super-spreading events in
440 Mycobacterium tuberculosis transmission: evidence from contact tracing. *BMC Infect Dis*.
441 2019;19:244.
- 442
- 443 23. California Department of Corrections and Rehabilitation. Population COVID-19 Tracking.
444 <https://www.cdcr.ca.gov/covid19/population-status-tracking/> (March 2, 2021, date last
445 accessed).
- 446
- 447 24. McCoy S, Bertozzi SM, Sears D, et al. Urgent Memo: COVID-19 Outbreak: San Quentin
448 Prison. 2020. Available at [https://amend.us/wp-content/uploads/2020/06/COVID19-](https://amend.us/wp-content/uploads/2020/06/COVID19-Outbreak-SQ-Prison-6.15.2020.pdf)
449 [Outbreak-SQ-Prison-6.15.2020.pdf](https://amend.us/wp-content/uploads/2020/06/COVID19-Outbreak-SQ-Prison-6.15.2020.pdf)

450

451 25. Wells WF. Air disinfection in day schools. *Am J Public Health*. 1943;33:1436-1443.

452

453 26. Thomas CJ. Measles in the Woolwich district. London County Council, Appendix to Report of
454 the Medical Officer of Health for London County Council for the Year 1904. 1905;46-60.

455 Available at <https://wellcomelibrary.org/item/b18252539>

456

457 27. Foster A, Kinzel, M. Estimating COVID-19 exposure in a classroom setting: A comparison
458 between mathematical and numerical models. *Phys Fluids*. 2021;33:021904

459

460 28. Chen PZ, Bobrovitz N, Premji Z, Koopmans M, Fisman DN, Gu FX. Heterogeneity in
461 transmissibility and shedding SARS-CoV-2 via droplets and aerosols [published online ahead
462 of print, 2021 Apr 16]. *Elife*. 2021;10:e65774

463

464 29. Edwards DA, Ausiello D, Salzman J, et al. Exhaled aerosol increases with COVID-19 infection,
465 age, and obesity. *Proc Natl Acad Sci USA*. 2021;118:e2021830118.

466

467 30. Goyal A, Reeves DB, Cardozo-Ojeda EF, Schiffer JT, Mayer BT. Viral load and contact
468 heterogeneity predict SARS-CoV-2 transmission and super-spreading events. *Elife*.
469 2021;10:e63537.

470